

Article

# Applying Circular Thermoconomics for Sustainable Metal Recovery in PCB Recycling

Jorge Torrubia <sup>1,2,\*</sup> , César Torres <sup>1,\*</sup> , Alicia Valero <sup>1</sup> , Antonio Valero <sup>1</sup> , Ashak Mahmud Parvez <sup>2</sup> ,  
Mohsin Sajjad <sup>2</sup>  and Felipe García Paz <sup>2</sup>

<sup>1</sup> Research Institute for Energy and Resource Efficiency of Aragón (Energia), University of Zaragoza, Campus Río Ebro, Mariano Esquillor Gómez, 15, 50018 Zaragoza, Spain; aliciavd@unizar.es (A.V.); valero@unizar.es (A.V.)

<sup>2</sup> Helmholtz-Zentrum Dresden—Rossendorf e.V. (HZDR), Helmholtz Institute Freiberg for Resource Technology (HIF), Chemnitz Str. 40, 09599 Freiberg, Germany; a.parvez@hzdr.de (A.M.P.); m.sajjad@hzdr.de (M.S.); felipe18\_93@hotmail.com (F.G.P.)

\* Correspondence: jtorrubia@unizar.es (J.T.); ctorres@unizar.es (C.T.)

**Abstract:** The momentum of the Fourth Industrial Revolution is driving increased demand for certain specific metals. These include copper, silver, gold, and platinum group metals (PGMs), which have important applications in renewable energies, green hydrogen, and electronic products. However, the continuous extraction of these metals is leading to a rapid decline in their ore grades and, consequently, increasing the environmental impact of extraction. Hence, obtaining metals from secondary sources, such as waste electrical and electronic equipment (WEEE), has become imperative for both environmental sustainability and ensuring their availability. To evaluate the sustainability of the process, this paper proposes using an exergy approach, which enables appropriate allocation among co-products, as well as the assessment of exergy losses and the use of non-renewable resources. As a case study, this paper analyzes the recycling process of waste printed circuit boards (PCBs) by disaggregating the exergy cost into renewable and non-renewable sources, employing different exergy-based cost allocation methods for the mentioned metals. It further considers the complete life cycle of metals using the Circular Thermoconomics methodology. The results show that, when considering the entire life cycle, between 47% and 53% of the non-renewable exergy is destroyed during recycling. Therefore, delaying recycling as much as possible would be the most desirable option for minimizing the use of non-renewable resources.

**Keywords:** thermoconomics; circular economy; renewable energies; PCB recycling; exergy life cycle; exergy replacement cost



**Citation:** Torrubia, J.; Torres, C.; Valero, A.; Valero, A.; Mahmud Parvez, A.; Sajjad, M.; García Paz, F. Applying Circular Thermoconomics for Sustainable Metal Recovery in PCB Recycling. *Energies* **2024**, *17*, 4973. <https://doi.org/10.3390/en17194973>

Academic Editor: George Halkos

Received: 29 July 2024

Revised: 17 September 2024

Accepted: 30 September 2024

Published: 4 October 2024



**Copyright:** © 2024 by the authors. Licensee MDPI, Basel, Switzerland. This article is an open access article distributed under the terms and conditions of the Creative Commons Attribution (CC BY) license (<https://creativecommons.org/licenses/by/4.0/>).

## 1. Introduction

The climate crisis and the Fourth Industrial Revolution are accelerating both the energy and digital transition [1–3], which, in turn, are driving up the demand for numerous metals and materials [4]. Some of these metals are copper, silver, gold, and palladium. For instance, these metals are found in almost all printed circuit boards (PCBs), which constitute the core of electrical and electronic equipment (EEE), including computers and data centers [5]. Additionally, copper is essential for renewable energies and the conduction of electricity, silver is used in significant quantities in silicon solar panels [6], and palladium is an essential metal in green hydrogen technologies [7]. However, these metals are not particularly abundant in nature, as evidenced by the progressive decrease in their ore grade since the beginning of the 20th century [8]. For instance, copper ore grades were about 2.5% in the early 20th century, decreasing to 0.6% by 2015 [9]. Because of this, it is essential to promote a circular economy capable of recovering metal resources from waste [4]. In the context of the digital transition, PCBs contained in waste electrical and electronic equipment (WEEE) are ideal candidates for resource recovery due to their high

concentration of valuable metals and their exponential growth in recent years, driven by the short lifespan of electronic devices [10]. However, recycling processes consume non-renewable resources, making it insufficient to simply recycle metals. It is more effective to do so using renewable energy sources in order to produce cleaner metals, supporting both the circular economy and the dual transition towards sustainability goals.

Life Cycle Assessment (LCA) is the most widely used methodology for analyzing the resources consumed and the environmental impacts of the production of metals such as copper [11–14]. However, this methodology presents several limitations. For instance, quality losses cannot be accurately measured using mass-based recovery methods, mass and energy balances may not be fully conserved, and the Life Cycle Impact Assessment (LCIA) remains a subjective and arbitrary step in current LCA methodologies [15,16]. These limitations could be addressed by incorporating exergy and exergy cost into the analysis. Exergy is the maximum theoretical useful work obtained if a system is brought into thermodynamic equilibrium with the environment, while the exergy cost reflects the cumulative exergy consumption required to manufacture a product throughout its life cycle [17]. The exergy cost allows for measuring the relationship between the material and energy dimensions through a single thermodynamic property, exergy [18]. An additional advantage of using exergy and exergy costs is that, as many of these metals will be used in the production of renewable energy during the energy transition, we can assess the contribution of materials in energy production in terms of non-renewable exergy [19]. Moreover, this approach allows us to incorporate the effect of raw material recovery into the analysis through a thermoeconomic assessment, a method widely used in energy systems [18], and now being applied to the evaluation of non-energy products.

In this respect, several studies have analyzed recycling from an exergy perspective [15,16,20–23], but they have not applied a thermoeconomic approach to distinguish between renewable and non-renewable exergy resources. Other research has focused on non-renewable exergy during the life cycle of products, but without a circular economy perspective [24,25]. This aspect is fundamental in the context of the energy transition since the use of renewable energies reduces the reliance on non-renewable resources for metal extraction. This reduction can be quantified by distinguishing the cost according to the origin of the energy source. Another problem arises when several metals are produced simultaneously since it is necessary to allocate exergy costs. LCAs commonly use economic allocation with a monetary approach [26,27]. However, prices are not a physical magnitude and are highly variable over time, making their use controversial [28]. In turn, the use of exergy criteria to allocate cost has several advantages [22,29], as will be shown in this paper.

This study applies a thermoeconomic analysis of the process of recycling copper, silver, gold, and palladium from waste PCBs. It compares different criteria for allocating resource costs based on embodied exergy. Additionally, the origin of the resources is considered, distinguishing between renewable and non-renewable sources. This approach allows for the evaluation of two scenarios: 2020 (using conventional fuels) and 2050 (using renewable fuels), for both primary and secondary production of the metals. Finally, analyzing the complete life cycle of metals enables us to assess and reflect on the efficiency of circularity through exergy.

## 2. Materials and Methods

Section 2.1 explains the thermoeconomic model for PCB recycling and the calculation of the recycling exergy cost for the four studied metals (Cu, Ag, Au, and Pd). These metals are the selected products of the recycling process since they concentrate most of the exergy cost of the production of the PCB. Section 2.2 provides the equivalent, but simplified, thermoeconomic assessment of the primary production of the metals, resulting in the calculation of the primary exergy costs for two scenarios: 2020 and 2050. Section 2.3 details the different criteria for allocating the exergy cost to each metal based on exergy methodologies.

### 2.1. Thermo-economic Analysis of PCB Recycling

The objective of the thermo-economic model is to evaluate the exergy cost of recycling metals (products) from PCBs (inputs), which need the consumption of energy, chemicals, and other materials. The exergy cost represents the cumulative exergy consumption necessary to manufacture a product, considering its life cycle, i.e., from the PCBs until the metals in this case. The thermo-economic analysis of the metallurgical simulation of PCB recycling is performed using the MATLAB package TaesLab 1.2 [30]. This software facilitates the thermo-economic analysis of industrial systems. TaesLab requires a data set to define the model:

- **Physical structure:** The physical structure represents the productive system, i.e., the physical connection between flows and processes. It is based on the metallurgical simulation shown in Figure 1 and Tables 1 and 2.
- **Productive structure:** The productive structure defines the function of each flow and process in the system. Flows can be resources (i.e., inputs of the model), intermediates (i.e., they connect two processes), outputs (i.e., the products of the system, in this case, the meals), or waste (i.e., the useless flows that leave the boundaries of the system). On the other hand, the processes are (1) productive, if their outputs are products or intermediate flows, or (2) dissipative, if their outputs are wastes. Thus, each flow is defined as a product or fuel depending on its function in the productive process. See Figure 2 and Table 2.
- **Thermodynamic model:** The thermodynamic model shows the set of equations (mass, energy, entropy balances...) that allow us to determine the exergy of the flows. They define the thermodynamic state of the plant.
- **Resources model:** It represents the external cost of the resources consumed by the plant.

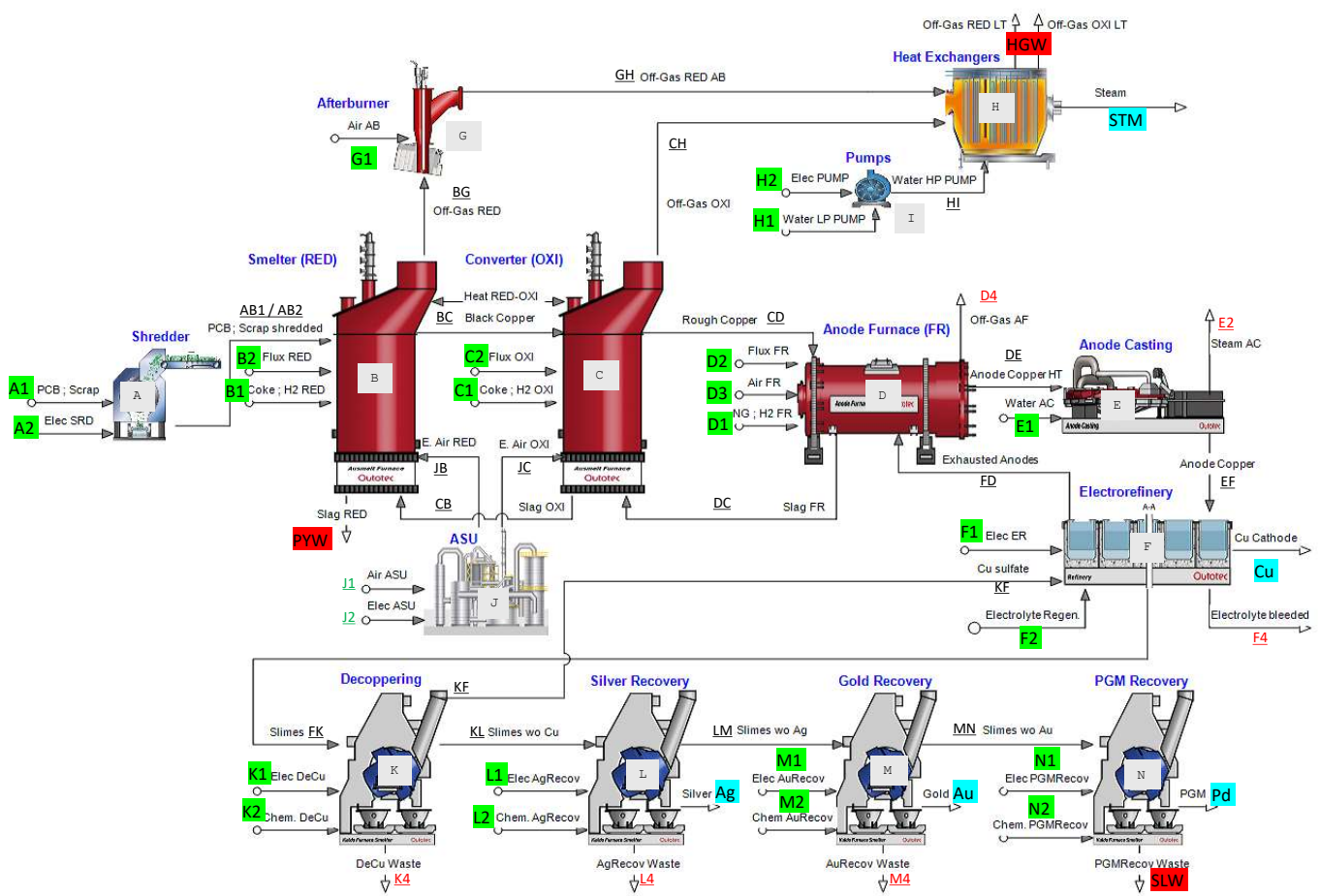


Figure 1. Block Flows Diagram of the PCB recycling process.

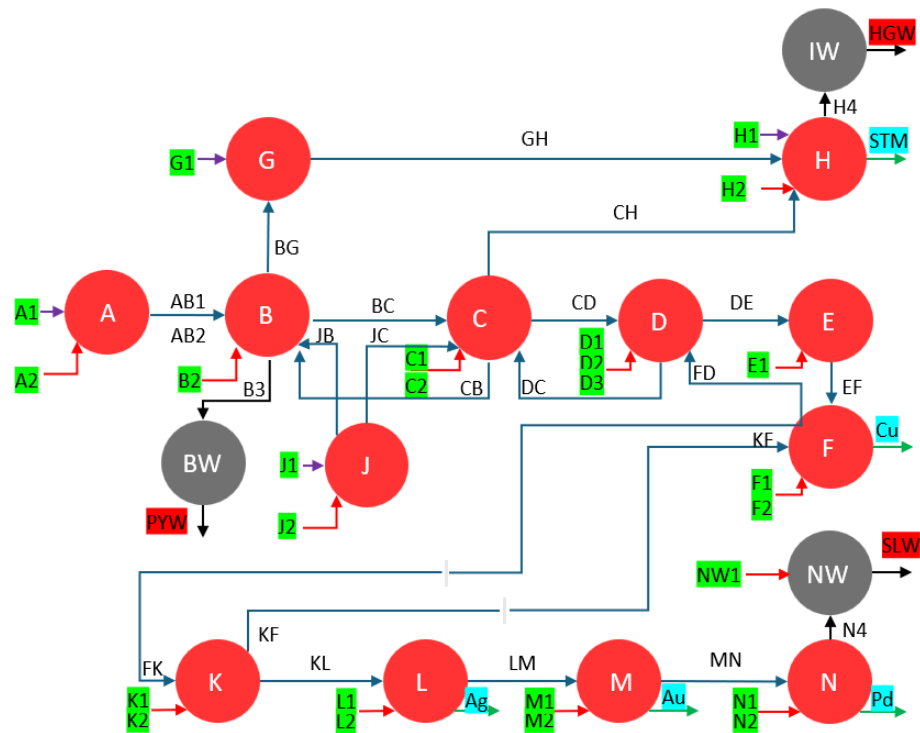


Figure 2. Thermoeconomic Diagram of the PCB recycling process.

Table 1. Flow Definition tables.

Resources	
Key	Description
A1	PCB Scrap
A2	Electricity Scarp
B2	Flux RED
C1	Coke-H2
C2	Flux OXI
D1	NG-H2
D2	Flux FR
D3	Air
E1	Cold Water
F1	Electricity ER
F2	Electrolite ER
G1	Air
H1	Electricity Pump
H2	Water
J1	Air
J2	Electricity ASU
K1	Electricity DeCu
K2	Chemical DeCu
L1	Electricity DeAg
L2	Chemical DeAg
M1	Electricity DeAu
M2	Chemical DeAu
N1	Electricity Pd
N2	Chemical Pd
NW1	Slimes treatment

Table 1. Cont.

Internal Flows	
Key	Description
AB1	PCB Shredder Plastic
AB2	PCB Shredder Metal
BC	Black Copper
BG	Heat Gases
B3	Slag RED
CB	Slag OXI
CD	Rough Copper
CI	Gases OXI
DC	Slag FR
DE	Anode Copper HT
EF	Anode Copper LT
FD	Exhausted Anode
FK	Slimes
H4	Hot Gases
GH	Heat Gases
JB	O2 Reduction
JC	O2 OXI
KF	Cu Sulphate (CuSO4)
KL	Slimes w/o Cu
LM	Slimes w/o Ag
MN	Slimes w/o Au
N4	Slimes not recovered
Outputs	
Key	Description
STM	Steam
Cu	Copper Cathode
Ag	Silver
Au	Gold
Pd	Palladium
Waste	
Key	Description
PYW	Pyrometallurgical waste
HGW	Hot Gases waste
SLM	Slimes waste

Table 2. Processes definition table.

Key	Description	Fuel	Product	Type
SRD	Shredding (A)	A1 + A2	AB1 + AB2	PRODUCTIVE
RED	Reduction (B)	(AB1 + JB – BG) + (B2 + AB2 + CB – B3)	BC	PRODUCTIVE
OXI	Oxidation (C)	C2 + (C1 + JC – CI) + (BC + DC – CB)	CD	PRODUCTIVE
FR	Fire Refining (D)	D1 + D2 + D3 + FD + (CD – DC)	DE	PRODUCTIVE
AC	Anode casting (E)	E1 + DE	EF	PRODUCTIVE
ER	Electrorefining (F)	F1 + F2 + KF + (EF – FD)	Cu + FK	PRODUCTIVE
AB	Afterburner (G)	G1 + BG	GH	PRODUCTIVE
HE	Heat exchanger (H)	H1 + H2 + (GH + C1eH4)	STM	PRODUCTIVE
ASU	Air separation unit (J)	J1 + J2	JB + JC	PRODUCTIVE
DeCu	Decoppering (K)	K1 + K2 + FK	KL + KF	PRODUCTIVE
AgRe	Silver recovery (L)	L1 + L2 + KL	Ag + LM	PRODUCTIVE
AuRe	Gold recovery (M)	M1 + M2 + LM	Au + MN	PRODUCTIVE
PdRe	Palladium recovery (N)	N1 + N2 + (MN – N4)	Pd	PRODUCTIVE
PYRW	Pyrometallurgical waste	B3	SLW	DISSIPATIVE
HEW	Heat exchanger waste	H4	HGW	DISSIPATIVE
SLMW	Slime waste	N4 + NW1	SLW	DISSIPATIVE

### 2.1.1. Physical Structure

The physical structure was obtained from [31,32], which uses the software HSC Chemistry 10 [33] to simulate the recovery of copper, silver, gold, and palladium from PCBs. Figure 1 represents the scheme obtained from HSC, and Figure 2 shows all the processes and flows for the thermoeconomic model. The differences between Figures 1 and 2 are the combination of pumps and the heat exchanger in a single process. The production diagram includes the dissipative equipment (shown in gray), whose function is to eliminate the residues produced in the entire production process: PYW (pyrometallurgical waste), HGW (thermal gas waste) and SLW (sludge waste). The costs of formation and disposal of these wastes are internalized and added to production costs. There are 16 processes (numbered A to N) and 55 flows.

### 2.1.2. Productive Structure

There are four types of flows, differentiated by color in Figure 2:

- Resources (Green): these are the input flows, which also have an associated exergy cost defined in the Resources Model. See Section 2.1.4
- Intermediate (Black): these flows connect two processes. In Figure 1, they are always identified with two letters. The first letter refers to its origin and the second letter to its destination.
- Output (Blue): these are the products, i.e., the recovered metals: copper (produced in electrorefining), plus silver, gold, and palladium, produced in precious metal recovery, besides the steam generated in the heat exchanger.
- Residues (Red): These are the wastes: slag from reduction, off-gases from reduction and oxidation, off-gases from fire refining, slimes from electrorefining, and slimes from the precious metal recycling process.

Table 1 describes the flows of the plant, grouped by flow type. Table 2 shows the purpose and efficiency of each process, indicating which flows are the product of the process and which flows constitute its fuel (resources). The fuel consists of:

- One or several inflows that provide exergy to the process.
- Flows that enter into the process and leave it after some exergy transfer to the process.

The product consists of the following:

- One or several outflows produced by the process.
- Flows that enter into the process and leave it, increasing its exergy.

There are two types of processes depending on their function inside the system:

- Productive: The products of these processes are internal flows (Internal) or final products (Output).
- Dissipative: The processes responsible for eliminating waste.

### 2.1.3. Thermodynamic Model

The exergies ( $B$ ) were calculated using HSC software from the mass flow rate, temperature and chemical composition of each stream. However, we extended the analysis using the exergy life cycle ( $ELC$ , calculated in Section 2.2) and the exergy replacement cost ( $ERC$ , obtained from [34], and further explained in Section 2.3). The exergy cost of metals from PCB recycling is allocated on the basis of these exergy models that depend on the limits of the system under consideration,  $ELC$  (current cost) or  $ERC$  (future cost), as explained in detail in Section 2.3. Table 3 shows the exergy of each flow depending on the allocation criterion used.

Table 3. Exergy Values of the thermodynamic model (kWh).

Key	Type	Scenario 2020			Scenario 2050		
		B	ELC	ERC	B	ELC	ERC
A1	RESOURCE	80,174	1,101,744	11,688,623	80,174	1,541,591	11,688,623
A2	RESOURCE	877.4	877.4	877.4	877.4	877.4	877.4
B2	RESOURCE	1551.6	1551.6	1551.6	3075.9	3075.9	3075.9
C1	RESOURCE	1976.8	1976.8	1976.8	3579.0	3579.0	3579.0
C2	RESOURCE	1517.7	1517.7	1517.7	1306.2	1306.2	1306.2
D1	RESOURCE	4455.2	4455.2	4455.2	3253.6	3253.6	3253.6
D2	RESOURCE	407.1	407.1	407.1	506.9	506.9	506.9
D3	RESOURCE	78.0	78.0	78.0	50.8	50.8	50.8
E1	RESOURCE	23.0	23.0	23.0	22.9	22.9	22.9
F1	RESOURCE	1426.1	1426.1	1426.1	1413.3	1413.3	1413.3
F2	RESOURCE	160.0	160.0	160.0	159.3	159.3	159.3
G1	RESOURCE	18.9	18.9	18.9	43.5	43.5	43.5
H1	RESOURCE	276.9	276.9	276.9	307.8	307.8	307.8
H2	RESOURCE	103.3	103.3	103.3	114.8	114.8	114.8
J1	RESOURCE	1030.2	1030.2	1030.2	1091.9	1091.9	1091.9
J2	RESOURCE	3471.0	3471.0	3471.0	-	-	-
K1	RESOURCE	23.0	23.0	23.0	23.0	23.0	23.0
K2	RESOURCE	10.4	10.4	10.4	10.4	10.4	10.4
L1	RESOURCE	22.5	22.5	22.5	22.5	22.5	22.5
L2	RESOURCE	5.8	5.8	5.8	5.8	5.8	5.8
M1	RESOURCE	45.4	45.4	45.4	45.4	45.4	45.4
M2	RESOURCE	20.6	20.6	20.6	20.6	20.6	20.6
N1	RESOURCE	24.5	24.5	24.5	24.5	24.5	24.5
N2	RESOURCE	13.1	13.1	13.1	13.1	13.1	13.1
NW1	RESOURCE	51.4	51.4	51.4	51.4	51.4	51.4
AB1	INTERNAL	66,178	66,178	66,178	66,178	66,178	66,178
AB2	INTERNAL	13,995	1,035,566	11,622,444	13,995	1,475,413	11,622,444
BC	INTERNAL	7366	1,054,384	11,780,363	6965	1,490,645	11,752,187
BG	INTERNAL	17,800	17,800	17,800	19,009	19,009	19,009
B3	INTERNAL	9494	11,208	20,574	12,151	14,457	26,319
CB	INTERNAL	5094	32,254	180,722	4674	29,242	155,614
CD	INTERNAL	3525	1,027,457	11,627,237	3404	1,465,021	11,613,083
CH	INTERNAL	683.9	683.9	683.9	1111.8	1111.8	1111.8
DC	INTERNAL	755.2	4829.1	27,098.4	855.1	3364.2	16,270.2
DE	INTERNAL	3643	1,176,477	13,340,609	3634	1,681,609	13,337,037
EF	INTERNAL	2924	1,175,759	13,339,890	2920	1,680,895	13,336,323
FD	INTERNAL	381.4	153,359	1,739,979	380.9	219,358	1,740,197
FK	INTERNAL	14.1	966,557	11,252,636	14.8	1,403,515	11,252,637
GH	INTERNAL	17,561.9	7561.9	17,561.9	18,696.1	18,696.1	18,696.1
H4	INTERNAL	5429.9	5429.9	5429.9	5417.8	5417.8	5417.8
JB	INTERNAL	708.5	708.5	708.5	691.4	691.4	691.4
JC	INTERNAL	50.0	50.0	50.0	61.0	61.0	61.0
KF	INTERNAL	4.9	110.7	688.8	4.9	116.2	688.8
KL	INTERNAL	7.3	966,445	11,251,946	7.3	1,403,396	11,251,946
LM	INTERNAL	2.5	896,226	11,213,139	2.5	1,298,435	11,213,139
MN	INTERNAL	1.9	155,859	9,994,760	1.9	170,453	9,994,760
N4	INTERNAL	0.5	11,777	92,926	0.5	17,296	92,926
STM	OUTPUT	8794.9	8794.9	8794.9	9775.6	9775.6	9775.6
Cu	OUTPUT	2421.8	54,775	340,955	2400.1	57,008	37,896
Ag	OUTPUT	4.8	70,218	38,806	4.8	104,961	38,806
Au	OUTPUT	0.6	740,366	1,218,379	0.6	1,127,981	1,218,379
Pd	OUTPUT	1.4	144,082	9,901,829	1.4	153,157	9,901,829
PYW	WASTE	9494.3	11,207.7	20,574.3	12,150.8	14,457.0	26,319.1
HGW	WASTE	5429.9	5429.9	5429.9	5417.8	5417.8	5417.8
SLW	WASTE	29.4	11,805.9	92,954.6	29.4	7325.0	92,954.6

#### 2.1.4. Resources Model

The *Resources Model* provides the exergy life cycle cost values of the resources disaggregated by the energy source, differentiating between non-renewable and renewable resources [17].

Figure 2 illustrates the resource type flows in green, while Tables A5 and A6 present the unit exergy cost values, i.e., the total exergy required (kWh) to obtain one kWh exergy entering the limits of the plant.

The main resources considered are as follows:

- PCB (A1): It represents the PCB waste to be recycled. Although the PCBs have already been amortized, the costs related to the collection, transport, and storage of PCBs should still be considered. However, since these costs are minimal compared to other resources, they have been assumed to be zero.
- Electricity (A2, F1, H2, J2, K1, L1, M1, N1): There are two electricity scenarios: 2020 and 2050. We obtained the data from [19].
- Fuel/Reducing Agent (C1, D1): These are coke, natural gas or hydrogen, depending on the scenario. The exergy cost of coke and natural gas are based on their Energy Return on Investment (EROI), and the exergy cost of hydrogen is calculated as described in [35].
- Flux (B2, C2, D2): Represents the exergy cost of producing fluxes composed of FeO, SiO<sub>2</sub>, or CaO in varying compositions, depending on whether they are used in reduction, oxidation, or refining. The exergy cost was calculated following the methodology described in [36].
- Chemicals (F2, K2, L2, M2, N2): Mainly sulfuric acid H<sub>2</sub>SO<sub>4</sub> for electrolysis, nitric acid HNO<sub>3</sub> used in Ag recovery, oxalic acid C<sub>2</sub>H<sub>2</sub>O<sub>4</sub> in Au recovery and ammonium chloride NH<sub>4</sub>Cl in PGM recovery. Their exergy cost was calculated following the methodology of [36].

Once the physical structure, the production structure, the thermodynamic model, and the resources model have been defined all the data are loaded into TaesLab [30] to obtain the results presented in the Section 3.

## 2.2. Thermoeconomic Analysis of the Primary Production of Metals

Circular thermoeconomics requires considering the entire life cycle of products, in this case, metals. For this reason, we have to determine the primary exergy cost of metals  $B_p^*$ , which refers to the exergy cost required from mineral extraction to the production of the final metal. It includes the effects of decreasing ore grade and the EROI of fossil fuels, representing the reduced net energy obtained due to the degradation of the fossil fuel deposits. Additionally, the life cycle of producing the electricity or hydrogen used to produce the metals is considered. We calculate three scenarios for  $B_p^*$ , due to the the energy transition: one scenario for 2020 and two scenarios for 2050 (one with renewable energies and the other with non-renewable energies). These three scenarios are used to compare the primary exergy cost with the recycling exergy cost results.

First, it is necessary to explain the calculation of the Exergy Life Cycle Cost (ELC) for the calculation of  $B_p^*$ . ELC represents the exergy cost but considers the electricity as final exergy. In other words, it does not account for the exergy cost of electricity production, which may vary depending on future developments in the energy transition. Figure 3 shows the disaggregation of the ELC into four stages: “Mining and concentration” (M&C), “Chemical production for mining and concentration” (M&C(CP)), “Smelting and Refining” (S&R), “Chemical production for Smelting and Refining” (S&R(CP)), and four fuels: “Natural gas”, “Oil”, “Coal”, “Electricity”, and the exergy of minerals. Figure 3 is equivalent to Figure 2 but for primary production. The main difference between them is that the complexity of the primary exergy cost calculation has been reduced as the processes were simplified from a previous study [36].

The exergy cost of the four steps and the four fuels for each metal was obtained from several sources [36–41], the chemical exergy of the minerals from [37], the energy cost from [36], and the procedure for the transformation of energy into exergy from [19]. These values are shown in Table A1. Furthermore, we considered the EROI degradation of fossil fuels from [38,39] and ore grade degradation from [8,40,41]. Considering these variables, the calculation of the exergy life cycle cost ELC for the year ( $yr$ ) ( $ELC_{yr}$ ), i.e., for 2020 or 2050, was performed through Equation (1).

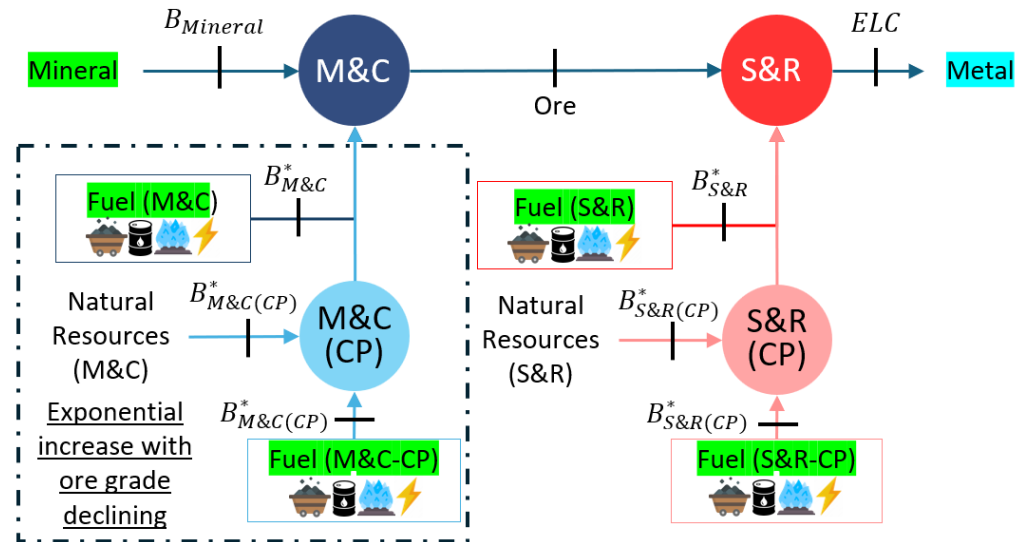


**Figure 3.** Thermo-economic Diagram of the primary production to obtain the Exergy life cycle cost (ELC) of a given metal. This figure is a simplified counterpart of Figure 2 for primary production.

$$\begin{aligned}
 ELC_{yr} = & B_{Mineral} + B_{NG-MC-yr}^* + B_{Oil-MC-yr}^* + B_{Coal-MC-yr}^* + B_{Elec-MC-yr}^* + \dots \\
 & B_{NG-MC(CP)-yr}^* + B_{Oil-MC(CP)-yr}^* + B_{Coal-MC(CP)-yr}^* + B_{Elec-MC(CP)-yr}^* + \dots \\
 & B_{NG-SR-yr}^* + B_{Oil-SR-yr}^* + B_{Coal-SR-yr}^* + B_{Elec-SR-yr}^* + \dots \\
 & + B_{NG-SR(CP)-yr}^* + B_{Oil-SR(CP)-yr}^* + B_{Coal-SR(CP)-yr}^* + B_{Elec-SR(CP)-yr}^*
 \end{aligned} \quad (1)$$

Equation (1) shows that all exergy cost variables  $B_{Fuel-step-yr}^*$  depend on the year under consideration (yr). However, the exergy cost of “Mining and Concentration” step  $B_{Fuel-MC-yr}^*$  and  $B_{Fuel-MC(CP)-yr}^*$  increases with time as a consequence of ore grade decline. This results in a higher exergy cost because a lower ore grade necessitates more exergy for mining and concentration. In turn, the exergy cost of the “Smelting and Refining” stages  $B_{Fuel-SR-yr}^*$  and  $B_{Fuel-SR(CP)-yr}^*$  remains unchanged, as a fixed-grade concentrate is produced regardless of the initial ore grade [42]. Therefore, the variation in the exergy cost for the “Smelting and Refining”  $B_{Fuel-SR-yr}^*$  is solely due to the decreasing EROI. On the other hand, to calculate the increase in the exergy costs of the “Mining and Concentration” step  $B_{Fuel-MC-yr}^*$ , Equation (2) is applied, in which we start from the current exergy cost  $B_{Fuel-step-C}^*$ , the current ore grade  $x_C$ , and the ore grade in any year  $x_{yr}^b$  and the exponent  $b$ , which is an experimental index that indicates how fast the ore grade decreases in the mine. The relationship between ore grade and years is based on several studies [8,41], and data are available in Table A2.

$$B_{Fuel-MC-yr}^* = B_{Fuel-MC-C}^* * (x_C / x_{yr}^b) \quad (2)$$

The trend of Equation (2) is shown qualitatively in Figure 4.

Once the ELC has been obtained, the primary exergy cost  $B_{P-yr}^*$  can be calculated with Equation (3) for the year 2020 and Equation (4) for the year 2050. We start from the (ELC), which is divided into fossil fuels  $ELC_{FF-yr}$  and electricity  $ELC_{ELEC-yr}$ . These are multiplied by the electricity cost of 2020  $B_{ELEC-2020}^*$  or 2050  $B_{ELEC-2050}^*$ , and by the cost of producing hydrogen only for the 2050 case. Thus, Scenario 2020 refers to the current energy mix, and Scenario 2050 assumes a strong penetration of renewable energies, according to the NZE scenario of the IEA [2].

$$B_{P-2020}^* = ELC_{FF-2020} + ELC_{Elec-2020} * B_{Elec-2020}^* \quad (3)$$

$$B_{P-2050}^* = ELC_{FF-2050} * B_{H2-2050}^* + ELC_{Elec-2050} * B_{Elec-2050}^* \quad (4)$$

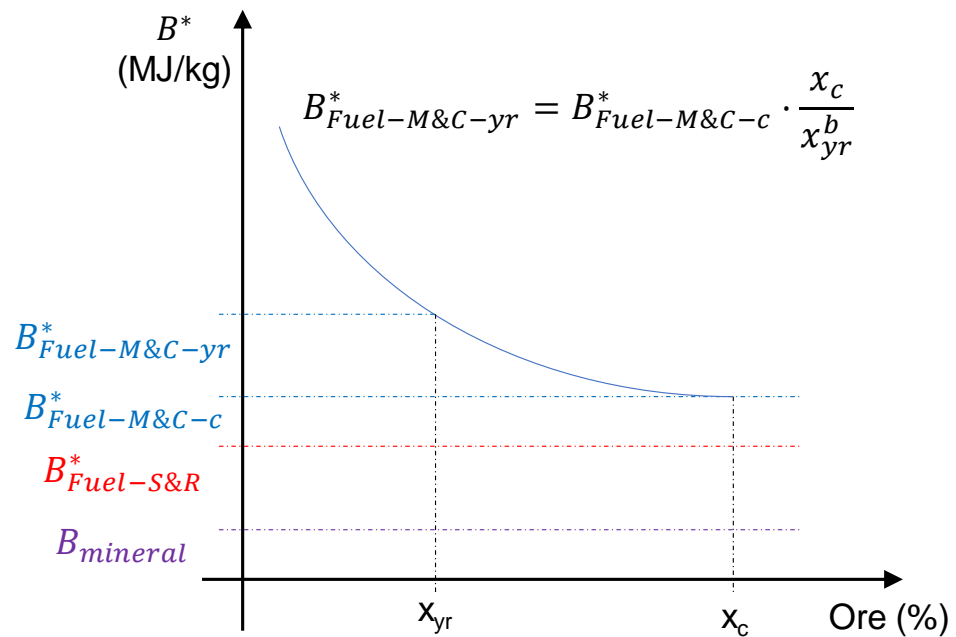


**Figure 4.** Exergy cost evolution as a function of ore grade decline.

### 2.3. Exergy Cost Allocation Methods

By means of the Circular Thermo-economic methodology [43], the amount, in exergy terms, required to obtain any flow of the plant or exergoecological cost could be calculated using Equation (5).

$${}^t\mathbf{C} = {}^t\mathbf{C}_e \langle \mathbf{B}^* \rangle, \quad (5)$$

where  ${}^t\mathbf{C}_e$  is the exergy life cycle cost of the resources,  ${}^t\mathbf{C}$  is the exergoecological cost of the system flows, and  $\langle \mathbf{B}^* \rangle$  is a matrix with dimensionless coefficients that depend on the definition of the productive structure and the exergy criteria used. The building up of this matrix is explained in [18]. This equation allows the costs of external resources to be allocated among the various final products based on physical criteria.

Table 3 shows the exergy values of the thermo-economic model under the three exergy methods analyzed in the paper:

- Exergy (B): This method allocates costs as a function of the exergy of the flows. In our case, the chemical exergy of the metals produced, obtained from [37]).
- Exergy Life Cycle Exergy Cost (ELC): This method uses the  $ELC_{2020}$  and  $ELC_{2050}$ , calculated through Equation (1). The difference between  $ELC_{2020}$  and  $ELC_{2050}$  is the increase in the exergy cost due to the decrease in ore grade, and EROI expected between 2020 and 2050 (see Figure 2). Thus, the ELC represents the exergy cost from the mineral extraction in the mine to its refining as a metal for a given ore grade and fossil fuel EROI. Consequently, it varies over time as both ore grade and EROI show a declining trend over time.
- Exergy Replacement Cost (ERC): This method uses ERC as a measure for allocation. The ERC represents the exergy required to extract and refine a mineral from a completely dispersed state in the Earth's crust, denoted as Thanatia [44], to its current average concentration in mines. It can thus be viewed as the bonus nature provides for having minerals concentrated in deposits rather than dispersed throughout the crust. The ERC is a constant value and gives greater weight to minerals that are scarce in the crust and energy-intensive to extract and refine. The ERC values were calculated by [34] and are the ones used in this paper.

The values of  $B$ ,  $ELC$ , and  $ERC$  for the metals analyzed in the paper are shown in Table A4. Using exergy ( $B$ ) as an allocation procedure is meaningful in energy production plants as their exergy content determines the value of the flows due to their role in generating energy. However, using this criterion for products whose purpose is not energy production is inconsistent. For instance, Table A4 shows that copper has 10 times more exergy than gold since it is more environmentally reactive than gold. However, gold is much scarcer (and more valuable) than copper. On the other hand,  $ELC$  shows the exergy destroyed during the metal production processes, and the  $ERC$  shows the exergy that will be destroyed if were are extracted from Thanatia, being a measure of the mineral scarcity [29]. Conclusively, physico-chemical exergy does not reflect the “usefulness” of metals, while  $ELC$  and  $ERC$  indicate the resources destroyed during the production process (either current  $ELC$  or future  $ERC$ ), so their use is more consistent.

The results allow us to establish the exergoecologic cost of Cu, Ag, Au, and Pd from recycling PCB or from primary production and discuss the different exergy allocations proposed ( $B$ ,  $ELC$ , or  $ERC$ ). Furthermore, it is possible to differentiate the portion of the exergy cost attributed to renewable versus non-renewable sources, depending on the chosen resources model, for the three scenarios considered, as outlined at the beginning of this section: Recycled 2020 scenario uses current conventional fuels (coke, natural gas, and 2020 electricity) and Recycled 2050 scenario uses alternative fuels, hydrogen, and renewable electricity [2].

### 3. Results and Discussion

First, we present the total exergy cost of metals for recycling and primary production under different exergy allocation criteria. Secondly, we present the total exergy cost of the previous section but disaggregated by the origin of the exergy, i.e., non-renewable or renewable. Finally, we illustrate the complete cycle of metals, assuming their use in PCBs, using Sankey diagrams to draw and highlight key conclusions about circularity.

#### 3.1. Recycling and Primary Exergy Cost of Metals

Table 4 compares the exergy costs of the metals obtained through the primary production  $B_p^*$  described in Section 2.2 and the costs of the metals obtained jointly in the recycling process  $B_R^*(B)$ ,  $B_R^*(ELC)$  and  $B_R^*(ERC)$ , which is described in Section 2.1. Regarding  $B_R^*$  results, since the total exergy cost of resources must be allocated to each product (Cu, Ag, Au, and Pd),  $B_R^*$  yields six different results depending on the exergy allocation criteria used (exergy ( $B$ ), exergy life cycle cost ( $ELC$ ) and Exergy Replacement Cost ( $ERC$ )) and the two scenarios (2020 and 2050). Regarding  $B_p^*$ , there are three different results: one for Scenario 2020: ( $B_p^*$ , which uses the current mix of energy, ore grade, and fossil fuel EROI, and two for Scenario 2050:  $B_p^*(NRE)$  and  $B_p^*(RE)$ .  $B_p^*(NRE)$  and  $B_p^*(RE)$  refer to the same ore grade and fossil fuel EROI for the year 2050, but  $B_p^*(NRE)$  maintains the same energy mix as in Scenario 2020, and  $B_p^*(RE)$  uses the energy mix of Scenario 2050.

**Table 4.** Exergy cost of metals depending on the allocation criterion (MJ/kg).

Key	Scenario 2020				Scenario 2050				
	$B_p^*$	$B_R^*(B)$	$B_R^*(ELC)$	$B_R^*(ERC)$	$B_p^*(NRE)$	$B_p^*(RE)$	$B_R^*(B)$	$B_R^*(ELC)$	$B_R^*(ERC)$
Cu	71	32.9	1.9	1.1	79	46	31.6	1.4	1.0
Ag	23,900	32.8	525.6	25.5	26,001	15,691	26.4	543.8	25.2
Au	529,534	94.1	14,159	2043	859,624	559,376	56.2	14,799	2,004
Pd	220,021	809.3	5842	33,536	247,851	209,101	484.6	4216	32,781

Table 4 shows the disadvantages of using the exergy criterion ( $B$ ) for the calculation of  $B_R^*$ . For instance, copper accounts for a very high portion of the cost (32.9–31.6 MJ/kg), showing even higher exergy costs than silver (32.8–26.4 MJ/kg). This is nonsense, as silver is much scarcer in nature than copper, and therefore, a higher share of the cost should be allocated it. For instance, Table 4 shows that  $B_p^*$  of silver is around 330 times higher than

copper, but these differences are inconsistent when compared with  $B_p^*(B)$ . This is because the chemical exergy of copper (2.09 MJ/kg) is double that of silver (0.92 MJ/kg). Therefore, the exergy criterion  $B$  is not a recommended method for calculating the physical cost of metals. Regarding ELC and ERC methods, the main difference is between the exergy cost of Au and Pd. Using ELC allocation, Au shows a higher exergy cost compared to Pd. However, when using ERC allocation, Pd exergy cost is higher than gold. This result is due to the very high ERC of Pd (8,983,377 MJ/kg) compared to the other metals Cu, Ag, and Au, as shown in Table A4. This high ERC is attributed to the significant scarcity of this element in nature. As explained in the methodology, the ELC is a variable cost that refers to the current exergy cost of the metal, while the ERC refers to the cost it will likely have in the future. Therefore, the preferred methods for cost allocation are *ELC* and *ERC*, discarding the  $B$  method for the rest of the analysis. Furthermore, recycling aims to save the exergy of primary production; therefore, it is consistent to consider the life cycle of metals for allocation through their exergy cost, either present *ELC* or future *ERC*.

From the point of view of metals, the savings between the exergy cost of primary production,  $B_p^*$ , and the exergy cost of recycling,  $B_R^*$ , are very high: around 97% using the ELC method and between 84% and 99% using the ERC method, depending on the metals. Therefore, recycling is always preferable to primary production. In addition, recycling offers other advantages, since it avoids the use of primary resources and thus prevents the ore grade of the deposits from decreasing. However, by focusing only on metals, we are not considering another intermediate exergy cost, such as the exergy required for PCB production. These exergy costs can be significant, and reduce the savings provided by recycling. This issue is discussed in Section 3.3.

Regarding the exergy cost of primary production  $B_p^*$ , we observe that by maintaining the energy mix constant, the exergy cost increases from  $B_p^*$  values in Scenario 2020 to  $B_p^*(NRE)$  in Scenario 2050, as both ore grade and fossil fuel EROI decrease in this period. However, if we consider a strong penetration of renewable energies in primary production  $B_p^*(RE)$ , we observe that the exergy cost is not only reduced compared to the use of non-renewable energies  $B_p^*(NRE)$ , but also compared to the ore grade and fossil fuel EROI in Scenario 2020 ( $B_p^*$ ). This is because renewable energies are far more efficient in the transformation of exergy than the conventional energy mix [36], and can counteract the effect of the decline in ore grade and fossil fuel EROI from 2020 to 2050.

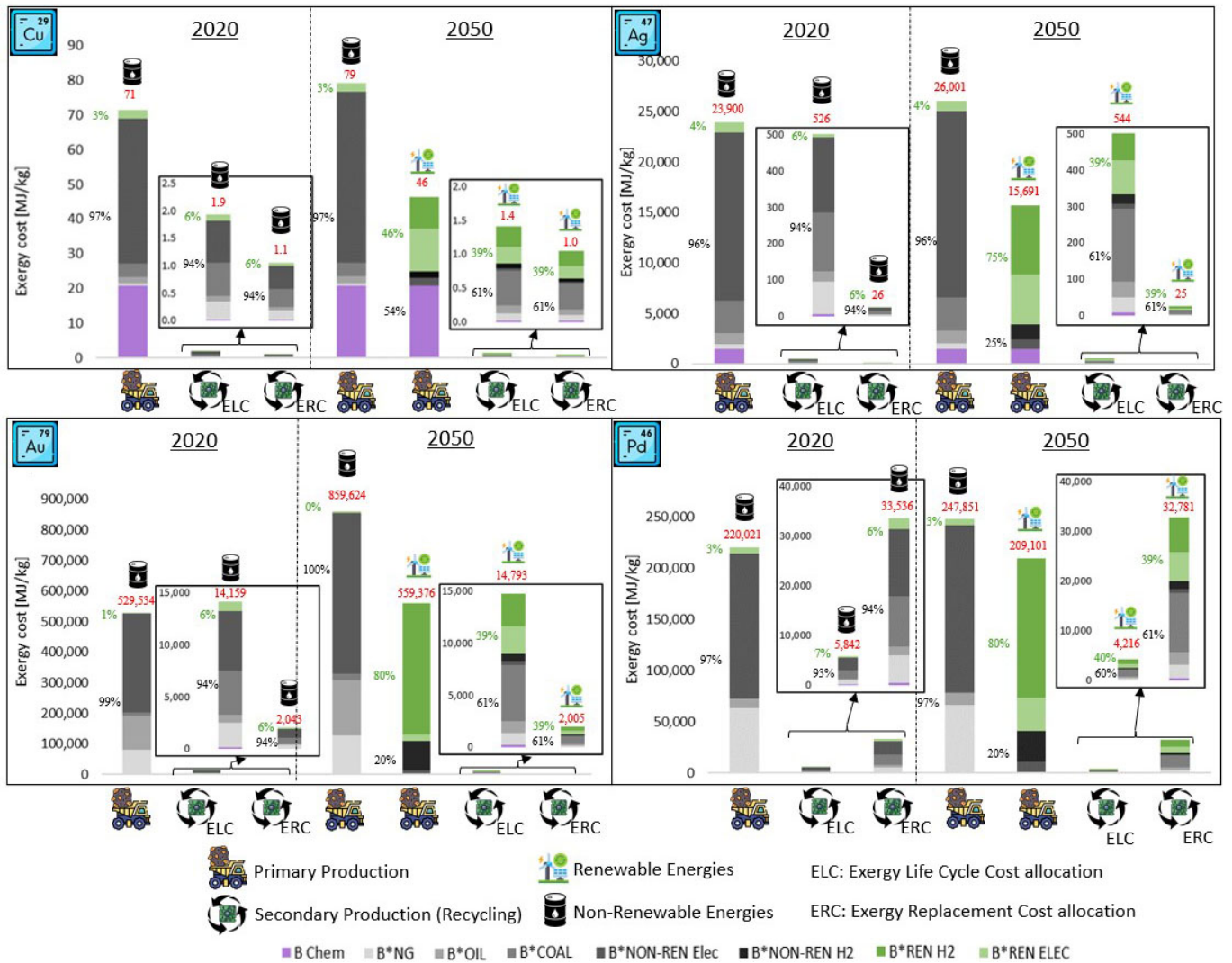
### 3.2. Non-Renewable and Renewable Exergy Cost of Metals

Figure 5 shows the exergy cost as presented in Table 4 for the four studied metals, for both recycling and primary production, disaggregated by the origin of the exergy. We excluded the exergy allocation ( $B$ ) because the most relevant allocations are *ELC* and *ERC*, as explained in the previous section. We divided the exergy into the chemical exergy of minerals ( $B_{ch}$ ), the exergy cost of natural gas, oil, and coal ( $B_{NG}^*$ ,  $B_{Oil}^*$ ,  $B_{Coal}^*$ , respectively), the non-renewable part of electricity and hydrogen ( $B_{NR}^*$ ), and the renewable part of the above ( $B_{RE}^*$ ).

All metals show very significant exergy savings when comparing recycling and primary production, as mentioned in Section 3.1. The difference in exergy costs is high enough to zoom into the graphs to see the recycling composition. Disaggregation allows us to analyze the savings in non-renewable exergy. Thus, in the case of copper, 23.2–76.1 MJ/kg of non-renewable exergy is saved with respect to primary production. In the case of silver, the savings are between 3310 and 25,011 MJ/kg of non-renewable exergy. Gold recycling saves between 96,249 and 854,313 of non-renewable exergy. Finally, recycled Pd saves between 9649 and 239,068 of non-renewable exergy. Saving non-renewable exergy should be the priority of recycling since it represents all resources that cannot be replaced by nature in a short timescale, for example, chemical exergy from minerals or fossil fuels.

The savings in non-renewable resources are also evident in primary production. Figure 5 shows two primary production scenarios for 2050: one that maintains the 2020 energy mix (NRE, since it is mostly non-renewable energy) and another that is based on the IEA-NZE scenario [2], with more renewables (RE). The comparison of these two scenarios allows

us to appreciate the effect of the decrease in ore grade (lower in 2020 than in 2020) on the increase in the non-renewable exergy costs of all metals when the energy mix is maintained (NRE scenarios). For example, it increases by 11.3% for Cu, 9.2% for Ag, 62.4% for Au, and 13.0% for Pd. However, considering the RE scenario, the non-renewable exergy cost decreases by 64% for Cu, 83% for Ag, 79% for Au, and 81% for Pd. The smaller decrease in the case of copper is due to the high chemical exergy of the mineral from which it is mainly obtained: chalcopyrite.



**Figure 5.** Disaggregated exergy cost of primary metals vs. recycling.

Using renewable energies in the recycling processes also reduces the cost of non-renewable energy. Thus, in the case of copper, the non-renewable exergy cost using *ELC* allocation (1.9 MJ/kg) is reduced from 1.8 MJ/kg to 0.9 MJ/kg, representing a decrease of 52%. Using renewable energies to recycle silver also shows a notable decrease in the non-renewable exergy cost of 32%. In the case of gold, the decrease in the exergy cost amounts to 32%, while for Pd, it is 54%.

Table 5 shows only the non-renewable exergy costs and their possible reduction from the worst-case scenario, represented by the primary extraction in 2050 using the current energy mix due to the lower ore grades. Table 5 considers the allocation scenarios with the exergy life cycle cost (*ELC*) and all metals studied. It shows that implementing renewable energies in primary extraction would reduce the non-renewable exergy cost between 67% and 87%. Copper would be the metal with the lowest reduction due to the high chemical exergy

of chalcopyrite that is destroyed in the production process. However, primary extraction would still require the extraction of natural resources from the mines, which would be depleted in the mining process, and their ore grade would decrease. Recycling would, therefore, save these resources for future generations. In addition, recycling, even with fossil technologies ( $B_R^*$  2020), would reduce the consumption of non-renewable resources even further, reaching reductions of 97.6% to 98.5%. However, the highest savings are obtained in the case of recycling using renewable energies. In this case, non-renewable exergy savings of 98.7% to 99.0% are achieved. Therefore, the most favorable cases are always those of recycling versus primary production, regardless of the energy sources used.

**Table 5.** Evolution of non-renewable exergy costs and metal savings for different scenarios.

	Cu		Ag		Au		Pd	
	$B_{NR}^*$ (MJ/kg)	Saving (%)						
$B_P^*$ [NR – 2050]	76.7	-	25,027	-	855,534	-	241,593	0.0
$B_P^*$ [RE – 2050]	25.0	67.4	3903	84.4	109,501	87.2	41,024	83.0
$B_R^*$ [ELC – 2020]	1.81	97.6	492	98.0	13,252	98.5	5452	97.7
$B_R^*$ [ELC – 2050]	0.86	98.9	333	98.7	9004	99.0	2524	98.9

### 3.3. Circular Thermoeconomics

Figures 6 and 7 show two Sankey diagrams showing the complete life cycle of the metals and materials embedded in PCBs, from their extraction in the mine to their recycling assessed, through the exergy cost (measured in kWh). The exergy cost is divided into its non-renewable and renewable contributions. Figure 6 shows the 2020 case, which uses conventional resources, while Figure 7 shows the 2050 scenario, which uses renewable resources in all stages. This vision focuses on the product, in this case, PCBs, and is different from that used in Sections 3.1 and 3.2, which focus on metals. Therefore, under this vision, it is not necessary to allocate the cost to the metals individually, and the intermediate stages of production of the product (PCBs) are considered. Therefore, the exergy cost of recycling (44,839 or 43,357 kWh) refers to the total exergy cost of recycling the 20 tons of PCBs. These figures correspond to 7.8 and 8.1 MJ/kg of PCB, comparable to the energy consumption of other references which range between 5.6 and 13.7 MJ/kg of PCB [45,46].

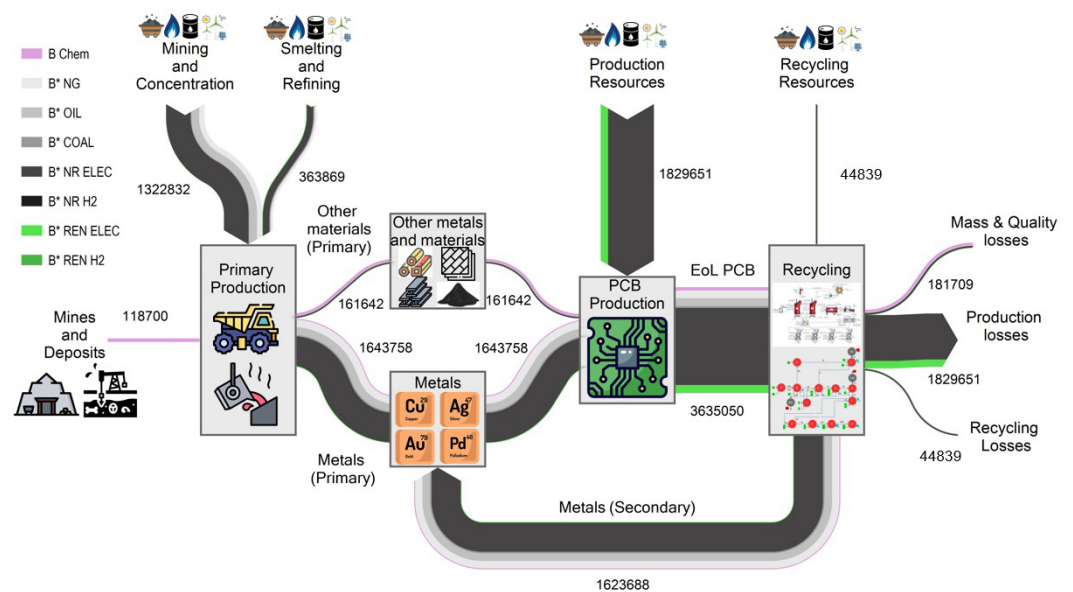


**Figure 6.** Sankey diagram of the complete life cycle of metals embedded in a PCB. Scenario 2020. Units in kWh.

The primary production stages distinguish between the chemical exergy from ores and fuels, the exergy cost of mining and concentrating the ores, and the smelting and refining exergy cost of transforming the ores into metals. We can observe that mining and concentrating costs are higher than smelting and refining. This is due to the significant contribution of gold mining, which accounts for 89% of the non-renewable exergy cost of this step. In the remaining metals (Cu, Ag, and Pd), the non-renewable exergy cost of smelting and refining represents the largest part: between 88.3% and 92.3%. On the other hand, chemical exergy from mines and deposits comes mainly from plastics embedded in PCBs (73%).

Once the metals and materials were produced, we distinguished between the exergy cost necessary to produce the four recycled metals: Cu, Ag, Au, and Pd, and the other metals and materials (see Figures 6 and 7). The metals selected for recycling (Cu, Ag, Au and Pd) comprise 91% of the entire non-renewable exergy cost, corresponding to 4.9% for Cu, 7.2% for Ag, 65.8% for Au, and 13.4% for Pd. Therefore, the recycling process is correctly focused since it can recover most of the exergy cost embodied in the PCB.

PCB production involves more resource consumption than raw materials since it is necessary to assemble all the components, such as integrated circuits, capacitors, and resistors. In this study, we have estimated the electricity needed for assembly at 87.5 kWh/kg of PCBs, obtained from the study of Yu et al. [47]. This exergy consumption is almost of the same magnitude as that required for the primary production of the materials, representing 47% of the total non-renewable energy cost of production, the remaining 53% being due to the production of materials. This fact has important implications since all this exergy is destroyed during recycling because obtaining a new PCB will require consuming it again.

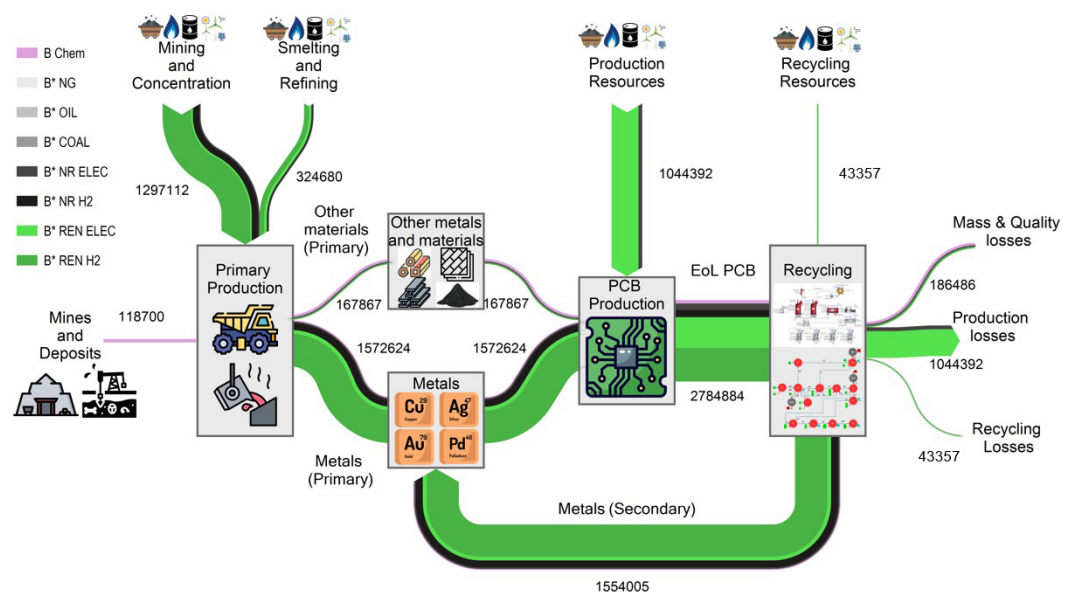


**Figure 7.** Sankey diagram of the complete life cycle of metals embedded in a PCB. Scenario 2050. Units in kWh.

Once the PCB is produced, used and reaches the end of its lifetime (EoL PCB), we consider that it is collected and transported to the recycling plant we discussed in this study. However, not all EoL PCBs end in plants suitable for recycling [48]. In fact, this is one of the main challenges for the circular economy, as much of the WEEE is either not collected or ends up in unknown locations [4].

Recycling processes always consume resources and produce losses. However, the non-renewable exergy cost of these losses is low compared to the non-renewable exergy embedded in the materials recovered. In the case of 2020, see Figure 6, the non-renewable exergy destruction during recycling accounts for 217,251 kWh (recycling losses plus mass and quantity losses) compared to 1,602,761 kWh embedded in the Cu, Ag, Au, and Pd recovered. Therefore, from the perspective of recycling alone, we observe that these

processes are highly efficient since only 10.7% of the non-renewable energy that enters the recycling process is destroyed. However, from this perspective, we are not considering PCB production losses. Therefore, we should consider all the intermediate steps between primary metal production and recycling since all the resource costs invested during PCB production will have to be consumed again in a new product cycle.

Hence, from a comprehensive circular economy perspective, recovering the 1,602,761 kWh of non-renewable exergy embedded in copper, silver, gold, and palladium results in a total destruction of 1,795,200 kWh. This includes losses due to mass and quality (9.8%), the exergy cost of recycling (2.3%), and the exergy cost of PCB production (87.9%). Therefore, when considering only the recycling perspective, 10.7% of non-renewable exergy is destroyed. However, when considering the complete life cycle, this exergy destruction amounts to 53%. In other words, in each circular economy cycle, more than half of the non-renewable resources are lost, despite considering 100% collection rates and having a process capable of recovering the most valuable metals (Cu, Ag, Au, and Pd), which make up 91% of the primary exergy cost of production.

One option to minimize the destruction of non-renewable exergy is to maximize the use of renewable energies in the primary production and recycling processes. However, renewable energies still carry a non-renewable exergy cost due to their life cycle [19]. This scenario is depicted in Figure 7. In this scenario, we observe a strong decrease in non-renewable exergy destroyed. Thus, the non-renewable exergy destroyed goes from 1,795,200 kWh in the 2020 case (Figure 6) to 287,211 kWh in the 2050 case (Figure 7), i.e., by using renewable energies, the non-renewable exergy cost is reduced by 84%. The distribution of these losses (287,211 kWh) differs from the 2020 case, with 45.2% coming from mass and quality losses, 45.9% from production, and 8.9% from recycling. The significant increase in mass and quality losses for the 2020 case (from 9.8% to 45.2%) is mainly because the recycling process uses plastics as fuel, and all its chemical exergy is lost in the process. On the other hand, as in the 2020 case, the percentage of exergy destruction throughout the life cycle remains significant. In the case of 2050, 287,211 non-renewable kWh are destroyed to recover the 326,281 kWh embedded in the materials, representing an efficiency of 47%.

In addition to recovering metals, steam is obtained during this process from the hot gases in the reduction and oxidation stages. The non-renewable unit exergy cost of the steam produced is 0.21 kJ/kJ and 0.16 kJ/kJ for the 2020 and 2050 scenarios, respectively, much lower than steam produced in a conventional steam boiler or a cogeneration plant driven by fossil fuels.

The important difference between considering a metal-centric approach (with savings between 97.6% and 99.0%, depending on the metal considered, Table 5) and product-centric approach [49] (with only savings of 47–53%, Figures 6 and 7), reinforces the importance of accounting for the entire life cycle of products (in this case a PCB) and of designing specific recycling processes that minimize the loss of non-renewable exergy. On the other hand, the high losses (47–53%) of non-renewable exergy during recycling indicate that these processes should be delayed as much as possible. Many measures can be promoted to achieve this: using fewer materials in production, intensifying product use, extending product lifetime, reuse, remanufacturing or refurbishing, among others. Thus, these results serve to measure the efficiency of the circular economy as a whole since losses during these processes are unavoidable. Therefore, the question arises as follows: to what extent is it possible to refer to a circular economy if it is necessary to destroy non-renewable energy in order to return materials to the economy, even when the use of renewable energy is maximized? Thus, Valero et al. [44] proposed the term Spiral Economy with the aim of raising awareness of the losses of exergy during these processes, as established by the Second Law of Thermodynamics.

#### 4. Conclusions

This work applies thermoeconomic analysis to study a PCB recycling process in which copper, silver, gold, and palladium are extracted. The methodology considers the complete

life cycle of PCBs from primary resource extraction to recycling using exergy as the currency to account for resource use. Three exergy-based cost allocation procedures are used to allocate costs during the recycling processes. Additionally, the exergy of the resources is decomposed into renewable and non-renewable, depending on their sources. In this way, we establish several scenarios for 2020 using conventional energy and 2050 using renewable energies, comparing their sustainability.

Of the three allocation procedures tested, those based on life cycle exergy cost and exergy replacement cost are the most reasonable, as they yield results that are closer to societal value perceptions of the metals. The life cycle exergy cost method has the advantage of reflecting the current situation but varies depending on the technologies used to produce the metals. In contrast, the exergy replacement cost method provides a constant value and offers a medium- to long-term perspective on the value of metals as they become depleted.

The worst-case scenario analyzed to obtain metals is primary extraction in 2050 using conventional energy. This is because the effect of ore grade and fossil fuel EROI decline are considered. Taking this scenario as a reference, it is possible to save between 67% and 87% of the non-renewable exergy cost just by applying renewable energies to primary production, despite the decrease in ore grade. The savings increase to 97.8–98.5% if metals come from recycled PCBs using conventional energies and up to 98.6–99.0% using renewable energies during recycling. However, when considering the point of view of the PCB, the destruction of non-renewable resources is much higher, ranging between 47% and 53% of the exergy cost saved in the recovered metals. These significant inefficiencies are mainly due to the exergy cost of PCB assemblage and the exergy losses due to the plastics used as fuel during the recycling process. This result underscores the importance of a product-centric perspective over a metal-centric perspective since each product has specific production processes that must be considered as losses during its life cycle, and recycling processes should be specifically designed for each product.

The objective of recycling should be to save non-renewable energy since it cannot be replaced by nature in a short time. On the other hand, renewable exergy, although also destroyed in the processes of transforming matter, can be replaced by nature since it ultimately originates from the Sun.

Thus, recycling not only conserves minerals from the Earth's crust but also helps preserve other non-renewable resources such as natural gas, oil, and coal. Exergy allows for the evaluation and comparison of all these resources using energy units. The example of PCBs in this work demonstrates that recycling should be delayed as much as possible in the product life cycle, as it invariably involves significant destruction of non-renewable resources. Measures such as reusing PCBs in other devices, salvaging their components, or separating plastics could delay recycling and reduce losses. The circular economy always involves exergy losses, as dictated by the Second Law of Thermodynamics. Therefore, terms like "Spiral Economy" might be more accurate, as spirals imply that cycles are not completely closed.

**Author Contributions:** Conceptualization, J.T., A.V. (Alicia Valero) and A.V. (Antonio Valero); Methodology, J.T., A.V. (Alicia Valero) and A.V. (Antonio Valero); Software, C.T.; Formal analysis, C.T.; Investigation, J.T.; Resources, M.S. and F.G.P.; Data curation, M.S. and F.G.P.; Writing—original draft, J.T.; Writing—review and editing, C.T. and A.M.P.; Supervision, A.V. (Alicia Valero); Funding acquisition, A.V. (Alicia Valero). All authors have read and agreed to the published version of the manuscript.

**Funding:** This research was funded by RESTORE project granted by Spanish Ministry of Science, Innovation and Universities (grant number PID2023-148401OB-I00) and Horizon Europe project REDOL (Grant Agreement 101091668).

**Data Availability Statement:** The original contributions presented in the study are included in the article, further inquiries can be directed to the corresponding authors.

**Conflicts of Interest:** The authors declare no conflicts of interest.

## Appendix A

This section shows all the data used in the methodology and a few complementary results. Table A1 shows all the initial data used for the calculation of  $ELC$  and  $B_p^*$  of the metals.

**Table A1.** Specific exergy values for primary extraction without considering ore grade and EROI declining (MJ/kg).

	Cu	Ag	Au	Pd
Exergy Minerals	20.7	1,510	0.0	193.0
NG_MC	0.0	36.6	48,600	0.0
OIL_MC	0.0034	278.0	77,200	7410
Coal_MC	0.0	113.0	5870	0.0
Elec_MC	3.94	1670	102,000	23,900
NG_MC_CP	0.104	24.4	8050	313.0
Oil_MC_CP	0.0114	5.37	882.0	130.0
Coal_MC_CP	0.0227	7.78	2690	18.8
Elec_MC_CP	0.0066	2.55	5490	45.2
NG_SR	0.53	173.0	0.0	59,500
Oil_SR	1.69	655.0	0.0	0.0
Coal_SR	3.52	2950	0.0	0.0
Elec_SR	9.71	3390	0.0	34,200
NG_SR_CP	0.0193	173.0	0.0	0.0
Oil_SR_CP	0.141	43.7	0.0	0.0
Coal_SR_CP	0.0049	21.60	0.0	0.0
Elec_SR_CP	3.45	1950	0.0	0.0
Exergy Cost	43.90	13,004	250,524	125,709

Table A2 shows the evolution of ore grade used for the years 2020 and 2050, used for the calculation of  $ELC$  and  $B_p^*$  of the metals.

**Table A2.** Ore grade evolution of minerals (kg/kg).

	Cu	Ag	Au	Pd
Ore grade ( $x_C$ )	$8.15 \times 10^{-3}$	$1.79 \times 10^{-4}$	$2.11 \times 10^{-6}$	$7.94 \times 10^{-7}$
Ore grade (2020)	$6.35 \times 10^{-3}$	$1.56 \times 10^{-4}$	$1.59 \times 10^{-6}$	$6.93 \times 10^{-7}$
Ore grade (2050)	$4.39 \times 10^{-3}$	$1.28 \times 10^{-4}$	$1.04 \times 10^{-6}$	$5.66 \times 10^{-7}$

Table A3 shows the amount (in kg) of PCBs introduced into the recycling process, as well as the amount of products produced for the recycling scenarios.

**Table A3.** PCB Recycling plant production values (kg).

Type	Product	Scenario 2020	Scenario 2050
Input	PCB	20,000	20,000
Output	Steam	19,127	21,260
Output	Copper	4178	4141
Output	Silver	19.80	19.80
Output	Gold	7.92	7.92
Output	Palladium	3.96	3.96

Table A4 compares the chemical exergy  $B_{ch}$ , exergy life cycle cost (ELC), and exergy replacement cost (ERC) of the analyzed metals.

**Table A4.** Chemical exergy, ELC for 2020 and 2050 scenarios, and ERC for the metals studied (MJ/kg).

	$B_{ch}$ [37]	ELC <sub>2020</sub>	ELC <sub>2050</sub>	ERC [34]
Cu	2.09	45	47	292
Ag	0.92	13,339	19,939	7371
Au	0.26	336,190	512,201	553,250
Pd	1.30	130,717	138,950	8,983,377

Tables A5 and A6 show the resource cost in kW/kW used in the recycling process for the years 2020 and 2050, respectively. The difference between the two tables is due to the higher integration of renewable energy in the year 2050. The exergy cost is divided according to the origin of the exergy as stated in the methodology. Table A7 shows in kWh the non-renewable exergy cost of each flow depending on the selected exergy allocation criteria: *B*, *ELC* or *ERC*.

**Table A5.** Cost of Resource streams for scenario 2020 (kW/kW).

Key	Mineral	NG	OIL	Coal	Elec-NR	H2-NR	Elec-RE	H2-RE	NR	RE	Total
A1	0.0000	0.0000	0.0000	0.0000	0.0000	0.0000	0.0000	0.0000	0.0000	0.0000	0.0000
A2	0.0000	0.0000	0.0000	0.0000	1.7907	0.0000	0.2856	0.0000	1.7907	0.2856	2.0763
B2	0.1316	0.5764	0.7117	2.7807	1.7348	0.0000	0.2767	0.0000	5.9353	0.2767	6.2120
C1	0.0000	0.0000	0.0000	1.0600	0.0000	0.0000	0.0000	0.0000	1.0600	0.0000	1.0600
C2	0.1459	0.6492	0.5768	3.5887	2.0496	0.0000	0.3269	0.0000	7.0102	0.3269	7.3371
D1	0.0000	1.0400	0.0000	0.0000	0.0000	0.0000	0.0000	0.0000	1.0400	0.0000	1.0400
D2	0.1459	0.6492	0.5768	3.5887	2.0496	0.0000	0.3269	0.0000	7.0102	0.3269	7.3371
D3	0.0000	0.0000	0.0000	0.0000	0.0000	0.0000	0.0000	0.0000	0.0000	0.0000	0.0000
E1	0.0000	0.0000	0.0000	0.0000	0.0000	0.0000	0.0000	0.0000	0.0000	0.0000	0.0000
F1	0.0000	0.0000	0.0000	0.0000	1.7907	0.0000	0.2856	0.0000	1.7907	0.2856	2.0763
F2	0.0000	0.0008	0.2457	0.0000	0.0598	0.0000	0.0095	0.0000	0.3063	0.0095	0.3158
G1	0.0000	0.0000	0.0000	0.0000	0.0000	0.0000	0.0000	0.0000	0.0000	0.0000	0.0000
H1	0.0000	0.0000	0.0000	0.0000	0.0000	0.0000	0.0000	0.0000	0.0000	0.0000	0.0000
H2	0.0000	0.0000	0.0000	0.0000	1.7907	0.0000	0.2856	0.0000	1.7907	0.2856	2.0763
J1	0.0000	0.0000	0.0000	0.0000	0.0000	0.0000	0.0000	0.0000	0.0000	0.0000	0.0000
J2	0.0000	0.0000	0.0000	0.0000	1.7907	0.0000	0.2856	0.0000	1.7907	0.2856	2.0763
K1	0.0000	0.0000	0.0000	0.0000	1.7907	0.0000	0.2856	0.0000	1.7907	0.2856	2.0763
K2	0.0000	0.0005	0.1581	0.0000	0.1384	0.0000	0.0221	0.0000	0.2970	0.0221	0.3190
L1	0.0000	0.0000	0.0000	0.0000	1.7907	0.0000	0.2856	0.0000	1.7907	0.2856	2.0763
L2	0.0000	0.8176	0.1042	3.6408	5.2194	0.0000	0.8326	0.0000	9.7819	0.8326	10.6145
M1	0.0000	0.0000	0.0000	0.0000	1.7907	0.0000	0.2856	0.0000	1.7907	0.2856	2.0763
M2	0.0000	4.7442	0.1177	0.1241	25.6890	0.0000	4.0977	0.0000	30.6751	4.0977	34.7728
N1	0.0000	0.0000	0.0000	0.0000	1.7907	0.0000	0.2856	0.0000	1.7907	0.2856	2.0763
N2	0.0000	3.2800	0.0235	1.8735	16.1314	0.0000	2.5732	0.0000	21.3084	2.5732	23.8816
NW1	0.0000	3.8847	0.0110	0.4451	8.9707	0.0000	1.4309	0.0000	13.3114	1.4309	14.7424

**Table A6.** Costs of Resource streams for scenario 2050 (kW/kW).

Key	Mineral	NG	OIL	Coal	El-NR	H2-NR	El-RE	H2-RE	NR	RE	Total
A1	0.0000	0.0000	0.0000	0.0000	0.0000	0.0000	0.0000	0.0000	0.0000	0.0000	0.0000
A2	0.0000	0.0000	0.0000	0.0000	0.1337	0.0000	0.9268	0.0000	0.1337	0.9268	1.0605
B2	0.1316	0.5764	0.7117	2.7807	0.1296	0.0000	0.8978	0.0000	4.3300	0.8978	5.2278
C11	0.0000	0.0000	0.0000	0.0000	0.0000	0.3232	0.0000	1.4638	0.3232	1.4638	1.7870
C12	0.0000	0.0000	0.0000	0.0000	0.0000	0.3232	0.0000	1.4638	0.3232	1.4638	1.7870
C2	0.1459	0.6492	0.5768	3.5887	0.1531	0.0000	1.0608	0.0000	5.1136	1.0608	6.1744
D1	0.0000	0.0000	0.0000	0.0000	0.0000	0.3232	0.0000	1.4638	0.3232	1.4638	1.7870
D2	0.1459	0.6492	0.5768	3.5887	0.1531	0.0000	1.0608	0.0000	5.1136	1.0608	6.1744
D3	0.0000	0.0000	0.0000	0.0000	0.0000	0.0000	0.0000	0.0000	0.0000	0.0000	0.0000
E1	0.0000	0.0000	0.0000	0.0000	0.0000	0.0000	0.0000	0.0000	0.0000	0.0000	0.0000
F1	0.0000	0.0000	0.0000	0.0000	0.1337	0.0000	0.9268	0.0000	0.1337	0.9268	1.0605
F2	0.0000	0.0008	0.2457	0.0000	0.0045	0.0000	0.0309	0.0000	0.2510	0.0309	0.2819
G1	0.0000	0.0000	0.0000	0.0000	0.0000	0.0000	0.0000	0.0000	0.0000	0.0000	0.0000
H1	0.0000	0.0000	0.0000	0.0000	0.0000	0.0000	0.0000	0.0000	0.0000	0.0000	0.0000
H2	0.0000	0.0000	0.0000	0.0000	0.1337	0.0000	0.9268	0.0000	0.1337	0.9268	1.0605
J1	0.0000	0.0000	0.0000	0.0000	0.0000	0.0000	0.0000	0.0000	0.0000	0.0000	0.0000
J2	0.0000	0.0000	0.0000	0.0000	0.1337	0.0000	0.9268	0.0000	0.1337	0.9268	1.0605
K1	0.0000	0.0000	0.0000	0.0000	0.1337	0.0000	0.9268	0.0000	0.1337	0.9268	1.0605
K2	0.0000	0.0005	0.1581	0.0000	0.0103	0.0716	0.0000	0.0000	0.2405	0.0000	0.2405
L1	0.0000	0.0000	0.0000	0.0000	0.1337	0.0000	0.9268	0.0000	0.1337	0.9268	1.0605
L2	0.0000	0.8176	0.1042	3.6408	0.3898	0.0000	2.7012	0.0000	4.9523	2.7012	7.6535
M1	0.0000	0.0000	0.0000	0.0000	0.1337	0.0000	0.9268	0.0000	0.1337	0.9268	1.0605
M2	0.0000	4.7442	0.1177	0.1241	1.9184	0.0000	13.2951	0.0000	6.9045	13.2951	20.1995
N1	0.0000	0.0000	0.0000	0.0000	0.1337	0.0000	0.9268	0.0000	0.1337	0.9268	1.0605
N2	0.0000	3.2800	0.0235	1.8735	1.2047	0.0000	8.3486	0.0000	6.3817	8.3486	14.7303
NW1	0.0000	3.8847	0.0110	0.4451	0.6699	0.0000	4.6427	0.0000	5.0107	4.6427	9.6533

**Table A7.** Non Renewable exergy cost of flows in PCB Recovery plant (kWh).

Key	Scenario 2020			Scenario 2050		
	B	ELC	ERC	B	ELC	ERC
A1	0.00	0.00	0.00	0.00	0.00	0.00
A2	1571.16	1571.16	1571.16	117.33	117.33	117.33
B2	9209.18	9209.18	9209.18	13,318.47	13,318.47	13,318.47
C1	2095.38	2095.38	2095.38	1156.90	1156.90	1156.90
C2	10,639.59	10,639.59	10,639.59	6679.64	6679.64	6679.64
D1	4633.36	4633.36	4633.36	1051.73	1051.73	1051.73
D2	2853.94	2853.94	2853.94	2592.33	2592.33	2592.33
D3	0.00	0.00	0.00	0.00	0.00	0.00
E1	0.00	0.00	0.00	0.00	0.00	0.00
F1	2553.73	2553.73	2553.73	189.00	189.00	189.00
F2	49.01	49.01	49.01	39.97	39.97	39.97
G1	0.00	0.00	0.00	0.00	0.00	0.00
H1	0.00	0.00	0.00	0.00	0.00	0.00
H2	185.00	185.00	185.00	15.36	15.36	15.36
J1	0.00	0.00	0.00	0.00	0.00	0.00
J2	6215.47	6215.47	6215.47	0.00	0.00	0.00
K1	41.15	41.15	41.15	3.07	3.07	3.07
K2	3.10	3.10	3.10	2.51	2.51	2.51
L1	40.38	40.38	40.38	3.02	3.02	3.02
L2	56.60	56.60	56.60	28.66	28.66	28.66
M1	81.38	81.38	81.38	6.08	6.08	6.08
M2	633.16	633.16	633.16	142.51	142.51	142.51
N1	43.80	43.80	43.80	3.27	3.27	3.27
N2	279.73	279.73	279.73	83.78	83.78	83.78
NW1	684.52	684.52	684.52	257.67	257.67	257.67
AB1	16,297.48	210.67	18.34	15,240.92	38.83	3.95
AB2	3446.58	3296.54	3221.52	3223.14	865.65	694.41
BC	46,226.91	17,319.95	16,943.31	33,734.90	14,357.88	14,172.20
BG	5882.10	1601.05	1549.87	4332.54	11.04	1.12
B3	21,189.91	136.64	22.12	22,543.71	138.71	31.72
CB	33,411.57	531.60	260.37	23,802.04	282.00	187.80
CD	32,885.68	29,298.35	29,121.56	24,254.47	21,618.67	21,507.40
CH	845.42	845.42	845.42	353.37	353.37	353.37
DC	7044.87	137.70	67.87	6093.21	49.64	30.13
DE	38,327.23	42,145.11	42,022.11	25,076.05	28,997.24	28,891.22
EF	38,327.23	42,145.11	42,022.11	25,076.05	28,997.24	28,891.22
FD	4999.12	5497.16	5481.12	3270.73	3784.15	3769.89
FK	208.73	37,149.67	37,994.81	134.99	24,450.93	24,612.73
GH	5882.10	1601.05	1549.87	4332.54	11.04	1.12
H4	2002.07	728.05	712.82	1281.68	99.67	96.96
JB	5805.55	5805.55	5805.55	0.00	0.00	0.00
JC	409.92	409.92	409.92	0.00	0.00	0.00
KF	101.39	4.26	2.33	56.34	2.02	1.51
KL	151.60	37,189.66	38,036.73	84.24	24,454.49	24,616.81
LM	83.91	34,577.53	38,002.19	39.13	22,654.82	24,563.47
MN	615.50	6137.51	34,509.91	144.71	2993.54	22,026.94
N4	150.96	463.76	320.85	35.49	303.76	204.79
STM	4910.45	1903.41	1867.46	3419.59	280.09	272.89
Cu	35,823.50	2105.27	1151.24	21,955.64	993.15	739.07
Ag	164.67	2709.11	131.52	76.78	1831.34	85.01
Au	182.94	29,154.55	4206.82	43.01	19,809.87	2685.12
Pd	788.07	5997.28	34,512.58	196.26	2776.83	21,909.19
PYW	21,189.91	136.64	22.12	22,543.71	138.71	31.72
HGW	2002.07	728.05	712.82	1281.68	99.67	96.96
SLW	835.49	1148.28	1005.38	293.16	561.42	462.46

## References

1. Xu, M.; David, J.M.; Kim, S.H. The fourth industrial revolution: Opportunities and challenges. *Int. J. Financ. Res.* **2018**, *9*, 90–95. [CrossRef]
2. International Energy Agency. Net Zero by 2050-A Roadmap for the Global Energy Sector. 2021. Available online: <https://www.iea.org/events/net-zero-by-2050-a-roadmap-for-the-global-energy-system> (accessed on 29 September 2024).
3. International Energy Agency. The Role of Critical Minerals in Clean Energy Transitions. 2021. Available online: <https://www.iea.org/reports/the-role-of-critical-minerals-in-clean-energy-transitions> (accessed on 29 September 2024).
4. Lallana, M.; Torrubia, J.; Valero-Delgado, A. Metals for energy & digital transition in Spain: Demand, recycling and sufficiency alternatives. *Resour. Conserv. Recycl.* **2024**, *205*, 107597. [CrossRef]
5. Forti, V.; Baldé, C.P.; Kuehr, R.; Bell, G. The Global E-waste Monitor 2020: Quantities, Flows and the Circular Economy Potential. United Nations University (UNU)/United Nations Institute for Training and Research (UNITAR)—Co-hosted SCYCLE Programme, International Telecommunication Union (ITU) & International Solid Waste Association (ISWA), Bonn/Geneva/Rotterdam. 2020. Available online: [https://ewastemonitor.info/wp-content/uploads/2020/11/GEM\\_2020\\_def\\_july1\\_low.pdf](https://ewastemonitor.info/wp-content/uploads/2020/11/GEM_2020_def_july1_low.pdf) (accessed on 29 September 2024).
6. Carrara, S.; Dias, P.A.; Plazzotta, B.; Pavel, C. *Raw Materials Demand for Wind and Solar PV Technologies in the Transition towards a Decarbonised Energy System*; Publications Office of the European Union: Luxembourg, 2020. Available online: <https://op.europa.eu/en/publication-detail/-/publication/19aae047-7f88-11ea-aea8-01aa75ed71a1/language-en> (accessed on 29 September 2024).
7. International Energy Agency. Energy Technology Perspectives 2023. Available online: <https://www.iea.org/reports/energy-technology-perspectives-2023> (accessed on 29 September 2024).
8. Mudd, G.M. The Sustainability of Mining in Australia: Key Production Trends and Their Environmental Implications for the Future. 2009. Available online: <https://users.monash.edu.au/~gmudd/files/SustMining-Aust-Report-2009-Master.pdf> (accessed on 29 September 2024).
9. Dong, D.; Van Oers, L.; Tukker, A.; Van Der Voet, E. Assessing the future environmental impacts of copper production in China: Implications of the energy transition. *J. Clean. Prod.* **2020**, *274*, 122825. [CrossRef]
10. Forti, V.; Balde, C.; Kuehr, R. E-Waste Statistics: Guidelines on Classification Reporting and Indicators, Second Edition. 2018. Available online: <https://www.itu.int/en/ITU-D/Environment/Pages/Toolbox/Guidelines.aspx> (accessed on 29 September 2024).
11. Chen, J.; Wang, Z.; Wu, Y.; Li, L.; Li, B.; Pan, D.; Zuo, T. Environmental benefits of secondary copper from primary copper based on life cycle assessment in China. *Resour. Conserv. Recycl.* **2019**, *146*, 35–44. [CrossRef]
12. Zhang, W.; Li, Z.; Dong, S.; Qian, P.; Ye, S.; Hu, S.; Xia, B.; Wang, C. Analyzing the environmental impact of copper-based mixed waste recycling—a LCA case study in China. *J. Clean. Prod.* **2021**, *284*, 125256. [CrossRef]
13. Zhang, J.; Tian, X.; Chen, W.; Geng, Y.; Wilson, J. Measuring environmental impacts from primary and secondary copper production under the upgraded technologies in key Chinese enterprises. *Environ. Impact Assess. Rev.* **2022**, *96*, 106855. [CrossRef]
14. Dong, D.; Tukker, A.; Steubing, B.; van Oers, L.; Rechberger, H.; Aguilar-Hernandez, G.A.; Li, H.; Van Der Voet, E. Assessing China’s potential for reducing primary copper demand and associated environmental impacts in the context of energy transition and “Zero waste” policies. *Waste Manag.* **2022**, *144*, 454–467. [CrossRef]
15. Amini, S.H.; Remmerswaal, J.A.; Castro, M.B.; Reuter, M.A. Quantifying the quality loss and resource efficiency of recycling by means of exergy analysis. *J. Clean. Prod.* **2007**, *15*, 907–913. [CrossRef]
16. Castro, M.B.; Remmerswaal, J.A.; Brezet, J.C.; Reuter, M.A. Exergy losses during recycling and the resource efficiency of product systems. *Resour. Conserv. Recycl.* **2007**, *52*, 219–233. [CrossRef]
17. Szargut, J. *Exergy Method—Technical and Ecological Applications*; WIT Press: Southampton, UK, 2005.
18. Torres, C.; Valero, A. The exergy cost theory revisited. *Energies* **2021**, *14*, 1594. [CrossRef]
19. Torrubia, J.; Valero-Delgado, A.; Valero, A. Renewable exergy return on investment (RExROI) in energy systems. The case of silicon photovoltaic panels. *Energy* **2024**, *304*, 131961. [CrossRef]
20. Ignatenko, O.; van Schaik, A.; Reuter, M.A. Exergy as a tool for evaluation of the resource efficiency of recycling systems. *Miner. Eng.* **2007**, *20*, 862–874. [CrossRef]
21. Ghodrat, M.; Samali, B.; Rhamdhani, M.A.; Brooks, G. Thermodynamic-based exergy analysis of precious metal recovery out of waste printed circuit board through black copper smelting process. *Energies* **2019**, *12*, 1313. [CrossRef]
22. Reuter, M.A.; Degel, R.; Borowski, N.; Apushkin, D. Digital twin for KGHM-Legnica: Simulation-based footprinting & exergy allocation of impacts. In Proceedings of the EMC 2023, Zrenjanin, Serbia, 16–17 June 2023.
23. Vierunketo, M.; Klemettinen, A.; Reuter, M.A.; Santasalo-Aarnio, A.; Serna-Guerrero, R. A multi-dimensional indicator for material and energy circularity: Proof-of-concept of exentropy in Li-ion battery recycling. *iScience* **2023**, *26*, 108237. [CrossRef] [PubMed]
24. Meester, B.D.; Dewulf, J.; Janssens, A.; Langenhove, H.V. An improved calculation of the exergy of natural resources for Exergetic Life Cycle Assessment (ELCA). *Environ. Sci. Technol.* **2006**, *40*, 6844–6851. [CrossRef] [PubMed]
25. Dewulf, J.; Bösch, M.E.; Meester, B.D.; Vorst, G.V.D.; Langenhove, H.V.; Hellweg, S.; Huijbregts, M.A. Cumulative exergy extraction from the natural environment (CEENE): A comprehensive life cycle impact assessment method for resource accounting. *Environ. Sci. Technol.* **2007**, *41*, 8477–8483. [CrossRef]

26. Lai, F.; Laurent, F.; Beylot, A.; Villeneuve, J. Solving multifunctionality in the carbon footprint assessment of primary metals production: Comparison of different approaches. *Miner. Eng.* **2021**, *170*, 107053. [[CrossRef](#)]
27. Farjana, S.H.; Huda, N.; Mahmud, M.A.P.; Saidur, R. A review on the impact of mining and mineral processing industries through life cycle assessment. *J. Clean. Prod.* **2019**, *231*, 1200–1217. [[CrossRef](#)]
28. Santero, N.; Hendry, J. Harmonization of LCA methodologies for the metal and mining industry. *Int. J. Life Cycle Assess.* **2016**, *21*, 1543–1553. [[CrossRef](#)]
29. Valero-Delgado, A.; Domínguez, A.; Valero, A. Exergy cost allocation of by-products in the mining and metallurgical industry. *Resour. Conserv. Recycl.* **2015**, *102*, 128–142. [[CrossRef](#)]
30. Torres, C.; Valero, A.; Valero-Delgado, A. TaesLab: An advanced software tool for circular thermoeconomics. In Proceedings of the ECOS 2024—The 36th International Conference on Efficiency, Cost, Optimization, Simulation and Environmental Impact of Energy Systems, Rhodes, Greece, 30 June–5 July 2024. [[CrossRef](#)]
31. Bassorgun, A. Precious Metal Recovery from Secondary Copper Anode Slimes Through Hydrometallurgical Route: A Study with Process Simulation and Life-Cycle Assessment Approach. Master's Thesis, Technische Universität Bergakademie Freiberg, Freiberg, Germany, 2023.
32. He, S. Precious Metal Recovery from Secondary Copper Anode Slimes: A Sensitivity Analysis Study Using Life Cycle Assessment Approach. Master's Thesis, Aalto University, Espoo, Finland, 2024. Available online: <https://urn.fi/URN:NBN:fi:aalto-202409086257> (accessed on 29 September 2024).
33. Outotec Research Center. HSC Chemistry 10, Thermochemical and Process Simulation. Available online: <https://hsc-chemistry.com/hscchemistry> (accessed on 29 September 2024).
34. Iglesias-Émbil, M.; Valero-Delgado, A.; Ortego, A.; Villacampa, M.; Vilaró, J.; Villalba, G. Raw material use in a battery electric car—A thermodynamic rarity assessment. *Resour. Conserv. Recycl.* **2020**, *158*, 104820. [[CrossRef](#)]
35. International Energy Agency. The Future of Hydrogen. Seizing Today's Opportunities. 2019. Available online: <https://www.iea.org/reports/the-future-of-hydrogen> (accessed on 29 September 2024).
36. Torrubia, J.; Valero-Delgado, A.; Valero, A. Energy and carbon footprint of metals through physical allocation. Implications for energy transition. *Resour. Conserv. Recycl.* **2023**, *199*, 107281. [[CrossRef](#)]
37. Valero-Delgado, A.; Valero, A.; Stanek, W. Assessing the exergy degradation of the natural capital: From Szargut's updated reference environment to the new thermoecological-cost methodology. *Energy* **2018**, *163*, 1140–1149. [[CrossRef](#)]
38. Hall, C.A.; Lambert, J.G.; Balogh, S.B. EROI of different fuels and the implications for society. *Energy Policy* **2014**, *64*, 141–152. [[CrossRef](#)]
39. Valero-Delgado, A.; Valero, A. What are the clean reserves of fossil fuels? *Resour. Conserv. Recycl.* **2012**, *68*, 126–131. [[CrossRef](#)]
40. Calvo, G.; Mudd, G.; Valero-Delgado, A.; Valero, A. Decreasing ore grades in global metallic mining: A theoretical issue or a global reality? *Resources* **2016**, *5*, 36. [[CrossRef](#)]
41. Der Voet, E.V.; Oers, L.V.; Verboon, M.; Kuipers, K. Environmental Implications of Future Demand Scenarios for Metals: Methodology and Application to the Case of Seven Major Metals. *J. Ind. Ecol.* **2019**, *23*, 141–155. [[CrossRef](#)]
42. Norgate, T.; Haque, N. Energy and greenhouse gas impacts of mining and mineral processing operations. *J. Clean. Prod.* **2010**, *18*, 266–274. [[CrossRef](#)]
43. Valero, A.; Torres, C. Circular Thermoeconomics. In *Advances in Thermodynamics and Circular Thermoeconomics*; WILEY: Hoboken, NJ, USA, 2024.
44. Valero-Delgado, A.; Valero, A.; Calvo, G. *The Material Limits of Energy Transition: Thanatia*; Springer Nature: Berlin/Heidelberg, Germany, 2024.
45. Fujita, T.; Ono, H.; Dodbiba, G.; Yamaguchi, K. Evaluation of a recycling process for printed circuit board by physical separation and heat treatment. *Waste Manag.* **2014**, *34*, 1264–1273. [[CrossRef](#)]
46. Navazo, J.M.V.; Méndez, G.V.; Peiró, L.T. Material flow analysis and energy requirements of mobile phone material recovery processes. *Int. J. Life Cycle Assess.* **2014**, *19*, 567–579. [[CrossRef](#)]
47. Yu, J.; Williams, E.; Ju, M. Analysis of material and energy consumption of mobile phones in China. *Energy Policy* **2010**, *38*, 4135–4141. [[CrossRef](#)]
48. Baldé, C.P.; D'Angelo, E.; Luda, V.; Deubzer, O.; Kuehr, R. Global Transboundary E-waste Flows Monitor. 2022. Available online: <https://ewastemonitor.info/gtf-2022/> (accessed on 29 September 2024).
49. Reuter, M.A.; van Schaik, A. Chapter 5-Material and product-centric recycling: design for recycling rules and digital methods. In *Handbook of Recycling*, 2nd ed.; Meskers, C., Worrell, E., Reuter, M.A., Eds.; Elsevier: Amsterdam, The Netherlands, 2024; pp. 79–95. [[CrossRef](#)]

**Disclaimer/Publisher's Note:** The statements, opinions and data contained in all publications are solely those of the individual author(s) and contributor(s) and not of MDPI and/or the editor(s). MDPI and/or the editor(s) disclaim responsibility for any injury to people or property resulting from any ideas, methods, instructions or products referred to in the content.